

Ferromagnetic-superconducting hybrid films and their possible applications: A direct study in a model combinatorial film

D. Stamopoulos, M. Pissas, and E. Manios

Institute of Materials Science, NCSR "Demokritos", 153-10, Aghia Paraskevi, Athens, Greece.

(Dated: March 22, 2024)

Model combinatorial films (CFs) which host a pure superconductor adjacent to a ferromagnetic-superconducting hybrid film (HF) are manufactured for the study of the influence of ferromagnetic nanoparticles (FNs) on the nucleation of superconductivity. Careful resistance measurements were performed simultaneously on two different sites of the CFs. Enhancement of superconductivity and magnetic memory effects were observed only on the hybrid site of the CFs but were absent on their purely superconducting part. Our results give direct proof that the FNs modulate the superconducting order parameter in an efficient and controlled way giving us the possibility of miscellaneous practical applications.

PACS numbers: 74.25.Fy, 74.78.Fk, 85.25.Hv

Ferromagnetic-superconducting hybrid systems where magnetism coexists with superconductivity have been the subject of intensive theoretical studies for many years.^{1,2,3,4} Advances in fabrication techniques have recently enabled the reliable preparation of such systems mainly in the form of HFs.^{5,6,7,8,9,10,11,12} Probably the HF which is most widely studied by recent experiments is the one consisting of ordered or randomly distributed FNs embedded in a superconducting layer.^{5,6,7,8,9,10,11,12} The most prominent effect that the FNs impose on the superconductor is the controlled modulation of the superconducting order parameter. Under specific conditions superconductivity in a HF may survive (or can be destroyed) at temperatures or magnetic fields higher (lower) than that observed in a single superconductor.^{5,6,7,8,9,10,11,12} In most studies transport measurements were mainly employed to probe the superconducting fraction of the HF. It was observed that under certain conditions, depending mainly on the alignment of the FNs, the resistance in the HF maintained a lower value than the one observed in a reference pure superconducting layer. Most of the studies attributed the lowering of the measured resistance to the enhancement of the bulk and/or the surface critical current that the superconductor may sustain.^{5,6,7,8,9,10,11,12} This specific property makes HFs important for power applications. Except for current-carrying applications HFs could be also useful as prototypes for the design of magnetoresistive memory devices or superconductive spin valves.^{13,14,15,16} In the near future such devices could serve as data storage elements in a similar way to other candidate devices which are based on different physical mechanisms (for example giant magnetoresistance elemental devices).

In this work we study the nucleation of superconductivity in model CFs which are constructed by CoPt FNs and a high quality layer of Nb superconductor. Nb and CoPt FNs were chosen as the ingredients of the CFs since their respective superconducting and magnetic properties are well studied and can be modified in a controlled way by altering the preparation conditions during sputtering and subsequent annealing.^{7,8,17,18,19} The FNs em-

ployed in this work are anisotropic with their easy-axis \hat{a}_e of magnetization normal to the surface of the film. In the constructed CFs the FNs are preferably embedded in only half of a high quality Nb layer of thickness $d = 200$ nm (see inset of Fig.2(b), below). In this way the modulation of the superconducting properties may be studied directly by performing resistance measurements on the HF and the pure superconducting areas of the CFs simultaneously under the application of the same dc transport current. The appearance of spatially modulated superconductivity and site selective memory effects give direct evidence that in the HF part of the CFs the nucleation of superconductivity can be greatly modulated by the dipolar fields of the FNs. The enhancement of the superconducting regime on the $H-T$ operational diagram suggests that such HFs could be attractive for current-carrying applications. In addition, a tristate superconducting magnetoresistive elemental device could be based on our CF.

Generally, the Nb layers are dc sputtered at a power of 57 W on a 2⁰⁰ pure Nb target and at an Ar pressure (99.999 % pure) of 3 m Torr.¹⁸ In the present study we managed to prepare films of even better quality by employing the following procedure. Since Nb is a strong absorber of oxygen, usually Nb oxide is grown along grain boundaries resulting in a suppression of the desired superconducting properties. In order to eliminate the residual oxygen that possibly existed in the chamber even after long periods (2–3 days) of pumping, we performed pre-sputtering for very long times. During the pre-sputtering process all the residual oxygen was absorbed by Nb. As a result we observed that after a pre-sputtering time of one hour the base pressure in the chamber was improved almost one order of magnitude exhibiting a typical value of $8 \cdot 10^{-8}$ Torr. Only when the desired base pressure had been obtained we started the actual deposition of the Nb layers.

The FNs employed in the present work were prepared as following. In order to induce a strong perpendicular anisotropy on the produced CoPt isolated particles a small quantity of Ag (typical thickness of the deposited

layer $d_{Ag} = 0.3 - 1.2$ nm) should be used as an extra underlayer.^{17,19} The Ag and CoPt layers were deposited on Si(001) substrates by magnetron sputtering at ambient temperature. The base pressure before introducing the Ar gas was 5×10^{-7} Torr and the pressure during sputtering was 3 mTorr. The nominal thickness of Ag layers for the CFs used in this work, was $d_{Ag} = 0.6$ nm and were sputtered by using a dc power of 5 W on a 2^{00} Ag target at a rate of 1.5 Å/sec. The nominal thickness of CoPt layers was $d_{CoPt} = 12$ nm and were sputtered by using an rf power of 30 W on a 2^{00} CoPt target at a rate of 1.2 Å/sec. This specific composition of $d_{Ag} = 0.6$ nm and $d_{CoPt} = 12$ nm was chosen for the deposited layers since it produces the most anisotropic FNs which in addition are isolated from each other.¹⁹ CoPt films deposited near room temperature adopt a disordered face centered cubic (fcc) structure which is magnetically soft. In order to form the hard magnetic and highly anisotropic L1₀ phase (ordered face centered tetragonal or fct) of CoPt, the as deposited films need to be annealed. Thus, the Ag/CoPt bilayers were annealed for 20 min at $T = 600$ °C under high vacuum (10^{-7} Torr). The annealing process leads to the formation of self-assembled anisotropic FNs. Their easy-axis \hat{a}_e of magnetization is normal to the surface of the film. As already discussed, morphologically, the FNs are isolated and randomly distributed on the substrate's surface as may be seen in Fig.1. Typical length scales (in-plane size and distance of the FNs) are in the range 100 - 500 nm. Cross-sectional transmission electron microscopy data (not shown) revealed that their thickness is of the order 30 - 50 nm. After producing the FNs the Nb layer was sputtered on top of them according to the procedure outlined above. The thickness of the deposited Nb layer is $d = 200$ nm. More specific information for the CoPt FNs may be found in Refs. 17,19.

Our magnetoresistance measurements were performed by applying a dc transport current (normal to the magnetic field) and measuring the voltage in the standard four-point configuration. In all measurements presented below the applied current was $I_{dc} = 0.5$ mA, which corresponds to an electric density $J_{dc} = 200$ A/cm² (typical in plane dimensions of the films are $1 - 4$ (mm)² to $4 - 4$ (mm)²). The temperature control and the application of the dc fields were achieved in a commercial SQUID device (Quantum Design). In all cases the applied field was parallel to the easy-axis \hat{a}_e of magnetization (H $\parallel \hat{a}_e$).

Figures 2 (a)-2 (c) show detailed voltage curves for two CFs as a function of temperature for various magnetic fields. The curves presented in Fig.2 (a) refer to the voltage $V_{1,4}(T)$ which was measured between the characteristic points 1 and 4. As is schematically presented in the inset of the middle panel these points are positioned on different sites of the CF. Point 1 is placed on the superconducting site, while point 4 is positioned on the HF part of the CF. Since the FNs are initially demagnetized, in zero magnetic field the voltage curve should not exhibit any special feature as indeed is evident in the data. Once again we note that by employing very long pre-sputtering

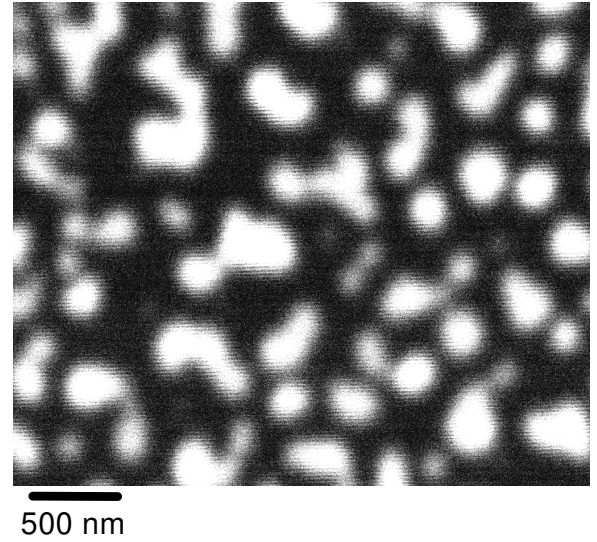


FIG. 1: Image of the FNs by scanning electron microscopy. The FNs are isolated and randomly distributed, while their typical in-plane size and their distance are in the range 100 - 500 nm.

times prior to the actual deposition we managed to produce high-quality Nb layers that maintain homogeneous superconducting properties throughout the CFs. This is evident by its high zero-field $T_c = 8.41$ K and the sharpness of its single-step transition which exhibits $T = 50$ mK according to a 10% - 90% criterion (see also Fig.4 below). In contrast to zero-field data, when an external magnetic field is applied the situation should alter dramatically due to the presence of the FNs in the HF part. As the external field is increased any modulation in the critical temperature of the HF, in respect to the adjacent Nb layer, should result in a structure in the measured curves $V_{1,4}(T)$ indicative of two different transitions. Indeed, this behavior is clearly observed in the data presented in Fig.2 (a). As we perform the measurements in higher external fields the voltage curves $V_{1,4}(T)$ broaden and gradually present a two step feature which indicates the two different transitions of the two different parts of the CF. More specifically, we observe that as the temperature decreases the $V_{1,4}(T)$ curves deviate from the normal state value at points $T_{ns}(H)$. In addition they exhibit first a change in their slope at a field-independent voltage level $V_{1,4}(T) \approx 80$ V (see horizontal dotted line tracing the points $T_{cs}(H)$) and second a sharp drop towards zero at a field dependent voltage level (see inclined dashed line tracing the points $T_{sd}(H)$). Finally, the CF becomes totally superconducting at points $T_z(H)$ where the resistance gets zero.

The direct comparison of $V_{1,4}(T)$ with $V_{3,4}(T)$ and $V_{1,2}(T)$ revealed that the upper part of the voltage curves $V_{1,4}(T)$ refers to the transition of the HF, while their lower part refers to the transition of the adjacent Nb layer. Representative data are shown in Fig.2 (b) where

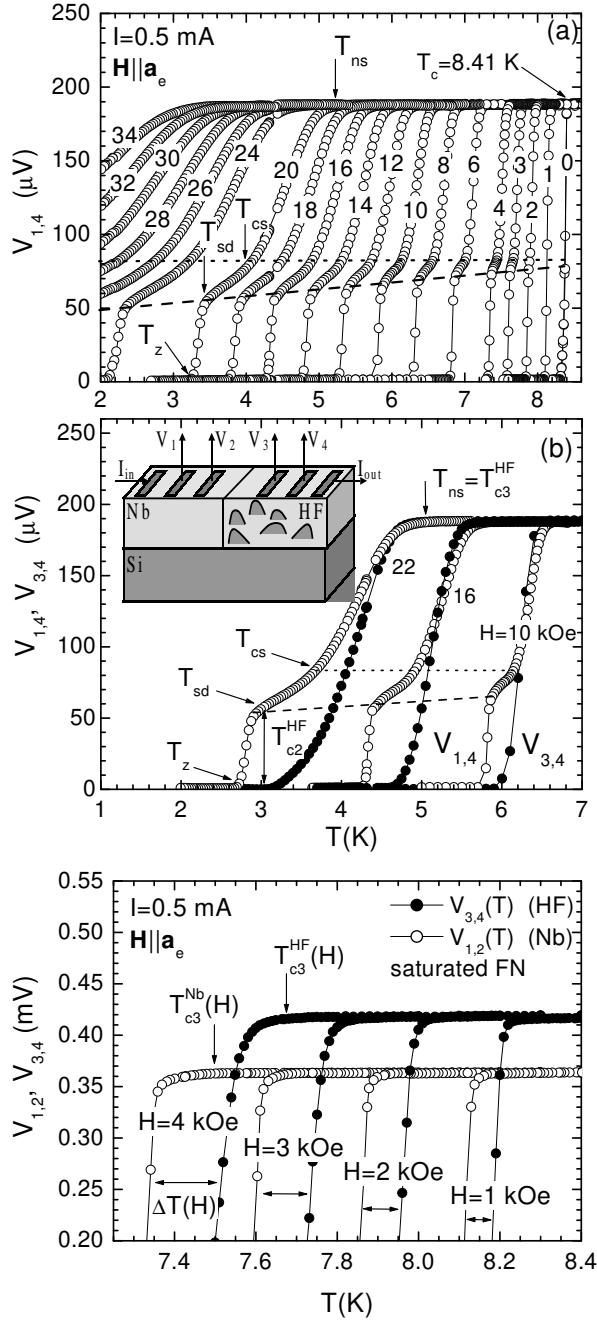


FIG. 2: (Upper panel) Detailed measurements of the voltage $V_{1,4}(T)$ (see the inset) for various magnetic fields 0 kOe H 34 kOe. (Middle panel) Comparative presentation of voltage curves $V_{1,4}(T)$ (open circles) and $V_{3,4}(T)$ (solid circles) at external magnetic fields $H = 10; 16$ and 22 kOe. The inset presents schematically the CF and the configuration of the performed measurements. (Lower panel) Comparative presentation of voltage curves $V_{1,2}(T)$ (open circles) and $V_{3,4}(T)$ (solid circles) measured in a second CF at low magnetic fields $H = 1; 2; 3$ and 4 kOe. In all cases the applied field was parallel to the magnetization easy-axis \hat{a}_e of the FNs.

we present comparatively the voltage curves $V_{1,4}(T)$ and $V_{3,4}(T)$ for magnetic fields $H = 10; 16$ and 22 kOe applied parallel to the easy-axis \hat{a}_e of magnetization of the FNs. First of all we see that as the temperature decreases both voltage curves $V_{1,4}(T)$ and $V_{3,4}(T)$ deviate from the normal state value at the same characteristic points $T_{ns}(H)$.²⁰ Second, the magnetically determined bulk upper-critical temperatures $T_{c2}^{HF}(H)$ of the HF part, represented by the zeroing of the $V_{3,4}(T)$ curves,^{7,8} nicely correlate with the points where the sharp drop in the voltage curves $V_{1,4}(T)$ initiates. We are now in a position to identify all four characteristic points existing in the $V_{1,4}(T)$ curves: The points $T_{ns}(H)$ where the normal state value is obtained refer to the points $T_{c3}^{HF}(H)$ where surface-like superconductivity starts to form in the HF part of the CF.^{7,8,21} The points $T_{sd}(H)$ where the sharp drop toward zero initiates (see inclined dashed line) are related to the bulk upper-critical temperatures $T_{c2}^{HF}(H)$ of the HF part. The zeroing temperatures $T_z(H)$ reflect the points $T_{c2}^{Nb}(H)$ where bulk superconductivity is established in the Nb part of the CF (then superconductivity is maintained in the whole CF) and finally the points $T_{cs}(H)$ where a change in the slope is observed in the $V_{1,4}(T)$ curves (see horizontal dotted line) refer to the temperatures $T_{c3}^{Nb}(H)$ where the pure Nb region of the CF enters the normal state as we increase the temperature.^{7,8} An important outcome of the data presented so far is that in the HF the superconducting transition takes place at higher temperatures than in the pure Nb area. In the lower panel, Fig 2(c) we focus near the normal state boundary of the $V_{1,2}(T)$ (open circles) and $V_{3,4}(T)$ (solid circles) voltage curves which were measured at the two different parts of a second CF. These data show clearly that, for the same applied magnetic field and current, the normal state boundary of the Nb part is placed at lower temperatures when compared to the HF part of the CF. Since all external experimental parameters (temperature, external magnetic field and applied current) are exactly the same for the Nb layer existing throughout the CF the enhanced superconducting temperature of its HF part should be attributed exclusively to the influence of the FNs.

The characteristic points discussed above are summarized in Fig 3 for the field configuration $H \parallel \hat{a}_e$. In its inset we present the initial part of the virgin magnetization loop of the CF performed at $T = 10$ K. The FNs of the present film exhibit a saturation field $H_{sat}^{FN} \sim 5$ kOe. In the main panel we observe that the line $H_{c3}^{HF}(T)$, which designates the normal state of the HF part of the CF, exhibits a change in its slope at the saturation field $H_{sat}^{FN} \sim 5$ kOe of the FNs.^{7,8,22} All other boundary lines referring to the different characteristic points don't exhibit such a tendency, but clearly maintain an almost linear behavior in the whole regime investigated in the present study. As a result the regime where the HF part of the CF maintains a resistance lower than the normal state value is significantly enhanced when compared to the respective regime of the pure Nb part. This finding is

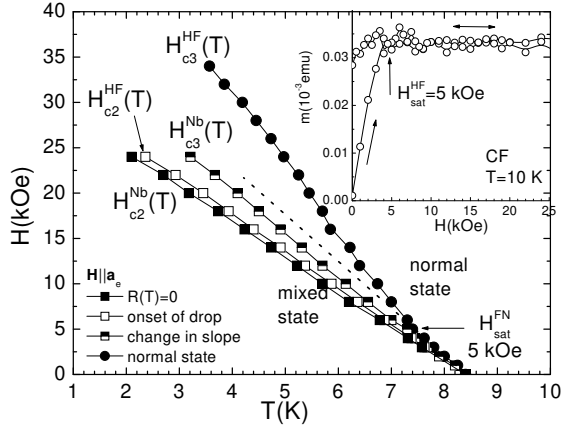


FIG. 3: The constructed phase diagram for the nucleation of superconductivity in our CF. The regime where the HF part of the CF maintains a resistance lower than the normal state value is greatly enhanced in comparison to the pure Nb part. This is achieved since an upturn is observed in $H_{c3}^{HF}(T)$ at the saturation field $H_{sat}^{HF} = 5$ kOe of the FNs (as may be seen in the inset where the initial part of a virgin loop performed at $T = 10$ K is presented). The dotted line represents the extrapolation of the low-field $H_{c3}^{HF}(T)$ data in high magnetic fields. The applied magnetic field was parallel to the easy-axis \hat{a}_e of magnetization ($H \parallel \hat{a}_e$).

in agreement to recent experimental studies performed in more simple HF's⁷ and suggests that by controlled variation of the saturation field of the FNs we may directly enhance the superconducting regime of the $H-T$ operational diagram.⁸ It should also be noted that the preparation procedure of randomly-distributed isolated FNs is much simpler compared to the techniques needed for the production of ordered ones. Thus, randomly distributed FNs could be more attractive for the construction of HF's that will be used for commercial current-carrying applications.

The presence of FNs should motivate magnetic memory effects in the superconducting properties of a HF. To investigate the existence of such phenomena in our model CF we performed measurements based on different magnetic histories of the FNs. Such data are presented in Figs. 4(a) and 4(b). In Fig. 4(a) solid points refer to the curves $V_{1,4}(T)$ obtained when the FNs were initially carefully demagnetized,²³ while the open points (positive fields) and points with crosses (negative fields) refer to $V_{1,4}(T)$ data obtained when initially the FNs were saturated by applying a magnetic field $H > H_{sat}^{FN} = 5$ kOe. We clearly see that in the temperature regime $T_{c2}^{HF}(H) < T < T_{c3}^{HF}(H)$ the voltage curves $V_{1,4}(T)$ are greatly affected by the magnetic state of the FNs, while their lower part $T_{c2}^{Nb}(H) < T < T_{c2}^{HF}(H)$ is left unchanged. This is so because the lower segment $T_{c2}^{Nb}(H) < T < T_{c2}^{HF}(H)$ of the curves is related to the transition of the pure Nb layer of the CF, while the upper segment $T_{c2}^{HF}(H) < T < T_{c3}^{HF}(H)$ reflects the transition of the HF part of the CF. Since the superconduct-

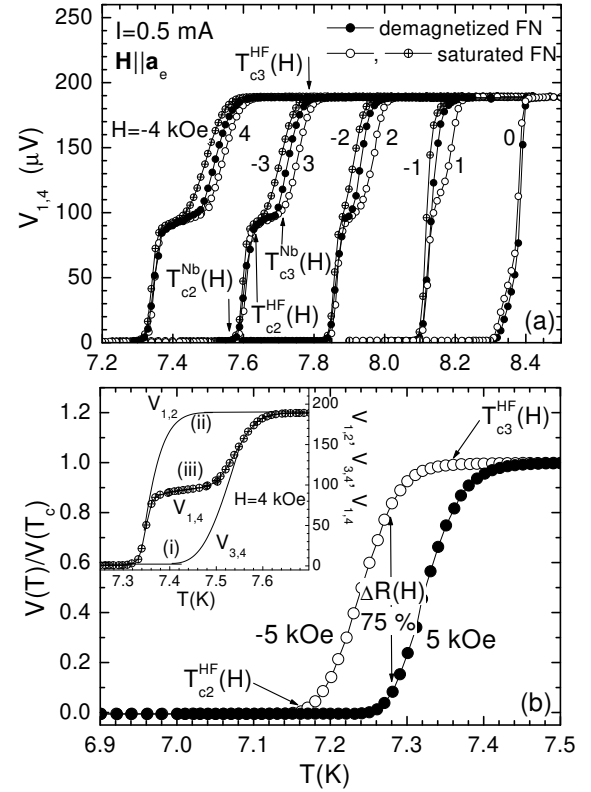


FIG. 4: (Upper panel) Voltage curves $V_{1,4}(T)$ at magnetic fields $H = 0; 1; 2; 3$ and 4 kOe after demagnetization (solid points) and after saturation (open points and points with crosses) of the FNs. Magnetic memory effects are observed in the $V_{1,4}(T)$ curves only in the temperature regime $T_{c2}^{HF}(H) < T < T_{c3}^{HF}(H)$, while their lower parts $T_{c2}^{Nb}(H) < T < T_{c2}^{HF}(H)$ coincide entirely. (Lower panel) Normalized voltage measured in a simple HF at $H = 5$ kOe. The observed change due to the change in the direction of the external field is $V(5\text{kOe}) = 75\%$. The inset presents schematically the three states of an elemental device which could be based on our CF. In all cases the magnetic field is parallel to the magnetization easy-axis \hat{a}_e of the FNs ($H \parallel \hat{a}_e$).

ing Nb layer extending in the whole CF is subjected to exactly the same extrinsic parameters (temperature, external magnetic field and applied current) it is only the FNs that could motivate the modulation of superconductivity and the magnetic memory effects observed in its HF part. We observe that the curves obtained at positive fields after the saturation of the FNs are placed in higher temperatures compared to the curves obtained when the FNs were initially demagnetized or the ones obtained at negative field values. This result clearly proves that the nucleation temperature of superconductivity can be modulated in a controlled way under the action of FNs.

In a recent Letter J.Y. Gu et al.¹⁶ have studied a HF multilayered device and reported a 25% resistance change which was motivated by the specific orientation of the magnetization of the magnetic layers. It should be

noted that in their multilayered HF the observed change in the resistance of the superconducting layer was not affected by the stray fields of the bordering magnetic layers but was motivated by the exchange-bias mechanism. In our HF the observed changes in the voltage are motivated by the stray fields of the FNs (see below). The data presented in Fig. 4 (b) were obtained in a simple HF when the external field was changed from $H = +5$ kOe to $H = -5$ kOe. A pronounced percentage change $V(-5\text{ kOe}) = 75\%$ is observed in the measured voltage which is motivated by the magnetic state of the FNs. Thus, a simple HF could probably serve as a convenient bistate magnetoresistive memory device. Furthermore, a CF could serve as a tristate memory device which, at constant temperature, exhibits three distinct resistive states as is schematically presented in the inset of Fig. 4 (b): (i) zero resistance (output at $V_{3,4}(T)$), (ii) normal state resistance (output at $V_{1,2}(T)$) and (iii) an intermediate value of the resistance (output at $V_{1,4}(T)$). Interestingly, the CF can be tuned between states (i), (ii) and (iii) under the application of an external field and more importantly its zero-resistance state (i) and intermediate state (iii) can be additionally modulated by the specific magnetic state of the FNs. This device could be considered as a development of the recently proposed magnetoresistive memory and superconducting spin-valve bistate elements.^{13,14,15,16} It should be noted that while the operation of those bistate elements^{13,14,15,16} is based on the exchange-bias mechanism our tristate elemental device simply works under the action of the dipolar fields of the FNs as discussed below (see also Refs. 6,7,8).

The modulation of superconductivity and the memory effects observed in our data may be explained by taking into account the contribution of the internal fields produced by the FNs.^{6,7,8,24} Briefly, these internal fields compensate (add to) the external field at some regimes of the superconductor where the two components are antiparallel (parallel).^{6,7,8,24} Since in these regimes the total effective magnetic field is lower (higher) than the external field superconductivity will survive (be destroyed) at temperatures higher (lower) than the ones observed in a single superconducting film.^{6,7,8,24} Thus, in our case when the FNs are initially demagnetized their influence on the superconducting layer is negligible. As the applied field increases the FNs are gradually oriented. Their dipolar fields reduce the external field in the areas of the superconductor which are placed near their lateral surfaces.^{6,7,8} As a consequence in these areas of the HF, superconductivity is preserved at temperatures higher than should be expected in the absence of FNs. Thus,

in our CF the nucleation of superconductivity should occur at higher temperatures in its HF part compared to the pure Nb part. This is directly observed in the results presented in Figs 2 and 4. Going a step further, we expect that different behavior should be observed in the case where the FNs were initially saturated by applying an external field $H > H_{\text{sat}}^{\text{FN}} \sim 5$ kOe and subsequently the field was decreased to the desired value where the measurement had to be performed. In this case, during the measurement all the FNs are in the remanent state throughout the HF area. As a consequence the suppression of the external magnetic field by the dipolar fields of the FNs in the areas adjacent to their lateral surfaces is now more efficient, and more importantly extends in the whole HF part. As a result, when the FNs are initially saturated superconductivity should be preserved at higher temperatures compared to the demagnetized initial state. This is clearly revealed by the data presented in Fig. 4 (a).

Since the discussed effect takes place mainly when all the FNs are aligned we speculate that at microscopic level the whole process relies on the formation of percolation paths that trace the lateral surfaces of the FNs in the whole HF's area. These paths assist the superconducting component of the transport current and as a result lower value of the resistance is maintained for higher temperatures in the HF part of a CF. Unfortunately, above the saturation field $H_{\text{sat}}^{\text{FN}} \sim 5$ kOe all the FN are saturated so that their ability to compensate the external magnetic field is entirely expended. As a consequence an increasing external field will gradually destroy superconductivity.

In summary, in this article we studied the nucleation of superconductivity in model CFs consisting of FNs preferably embedded at the half part of a high quality Nb layer. Resistance measurements were performed simultaneously at the HF and the purely superconducting regimes of the CFs under the application of the same transport current. Under the presence of an external magnetic field in the HF regime superconductivity is preserved at temperatures higher than that observed in the pure superconducting area of the CFs. Magnetic memory effects are selectively observed only in the HF part but are absent in the pure superconducting regime. Our results show that in a HF we are able to greatly enhance the superconducting regime of the $H-T$ operating diagram thus making a superconductor more attractive for current-carrying applications. Finally, our CF could be considered as a tristate elemental magnetoresistive unit and may be useful for the design of oncoming memory devices.

¹ A. I. Buzdin, L. N. Bulavskii, and S. V. Panyukov, Zh. eksp. Teor. Phys. 87, 299 1984 [Sov. Phys. JETP 60, 174 (1984)].

² A. I. Buzdin and A. S. Mel'nikov, Phys. Rev. B 67, 020503(R) (2003).

³ A. Yu. Ladyshkin, A. I. Buzdin, A. A. Fraerman, A. S.

Mel'nikov, D. A. Ryzhov, and A. V. Sokolov, Phys. Rev. B 68, 184508 (2003).

⁴ J. Aarts, J. M. E. Geers, E. Brck, A. A. Golubov, and R. Coehoorn, Phys. Rev. B 56, 2779 (1997).

⁵ D. J. M. organ and J. B. Ketterson, Phys. Rev. Lett. 80, 3614

- (1998).
- ⁶ Martin Lange, Margriet J. Van Bael, Yvan Bruynseraede, and Victor V. Moshchalkov, Phys. Rev. Lett. 90, 197006 (2003).
 - ⁷ D. Stamopoulos, M. Pissas, E. Karanasos, D. Niarchos, and I. Panagiotopoulos, Phys. Rev. B 70, 054512 (2004).
 - ⁸ D. Stamopoulos and E. Manios, to be submitted.
 - ⁹ J.I. Martin, M. Velez, J. Nogues, and Ivan K. Schuller, Phys. Rev. Lett. 79, 1929 (1997).
 - ¹⁰ O.M. Stoll, M.I. Montero, J. Guimpel, Johan J. Akerman, and Ivan K. Schuller, Phys. Rev. B 65, 104518 (2002).
 - ¹¹ J.E. Villegas, E.M. Gonzalez, M.I. Montero, Ivan K. Schuller, and J.L. Vicent, Phys. Rev. B 68, 224504 (2003).
 - ¹² A. Terentiev, D.B. Watkins, L.E. DeLong, D.J. Morgan, and J.B. Ketterson, Physica C 324, 1 (1999).
 - ¹³ Sangjun Oh, D. Youm, and M.R. Beasley, Appl. Phys. Lett. 71, 2376 (1997).
 - ¹⁴ L.R. Tagirov, Phys. Rev. Lett. 83, 2058 (1999).
 - ¹⁵ A.I. Buzdin, A.V. Vedyayev, and N.V. Ryzhanova, Europhys. Lett. 48, 686 (1999).
 - ¹⁶ J.Y. Gu, C.-Y. You, J.S. Jiang, J. Pearson, Ya.B. Bazaliy, and S.D. Bader, Phys. Rev. Lett. 89, 267001 (2002).
 - ¹⁷ V. Karanasos, I. Panagiotopoulos, D. Niarchos, H. Okumura, and G.C. Hadjipanayis, Appl. Phys. Lett. 79, 1255 (2001).
 - ¹⁸ D. Stamopoulos, A. Speliotis, and D. Niarchos, Supercond. Sci. Technol. 17, 1261 (2004).
 - ¹⁹ E. Manios, V. Karanasos, D. Niarchos, and I. Panagiotopoulos, J. Magn. Magn. Mater. 272-276, 2169 (2004).
 - ²⁰ In Fig.2(b) it appears that, for $H = 10$ and 16 kOe, $V_{3,4}(T) > V_{1,4}(T)$ near their onset point, while from its schematic inset it is expected that $V_{3,4}(T) < V_{1,4}(T)$ should always hold. This fact is not actual, but factitious. During our measurements only the curves $V_{1,2}(T)$ and $V_{3,4}(T)$ could be measured simultaneously. The measurements of the curves $V_{1,4}(T)$ were performed in different scans. Thus, the observed irregularity is related to a small relative temperature shift between $V_{3,4}(T)$ and $V_{1,4}(T)$ due to the slightly different values of the applied magnetic field during different measurements (no-overshoot operation mode of the SQUID). The data presented in Fig.2(c), that were obtained when $V_{1,2}(T)$ and $V_{3,4}(T)$ were measured simultaneously, leave no doubt for the validity of our results.
 - ²¹ Since the $I-V$ characteristics are non-linear in the regime $T_{c2}^{Nb}(H) < T < T_{c3}^{HF}(H)$ we attribute this regime to surface superconductivity (data not shown here but may be found in Refs.7,8).
 - ²² A second gradual change in the slope of $H_{c3}^{HF}(T)$ line which is observed around 20 kOe is not related to any magnetic characteristic of the FNs. We believe that it is related to the conventional curvature expected as zero temperature is approached.
 - ²³ Demagnetization takes place at $T = 10$ K $> T_c = 8.41$ K by performing sequential loops while decreasing the maximum value of the applied magnetic field. After this procedure is completed the net magnetic moment of the FN is $m < 5 \cdot 10^6$ emu.
 - ²⁴ Sa-Lin Cheng and H.A. Fertig, Phys. Rev. B 60, 13107 (1999).